AD A135 155 PROGRAM ON ELECTRICALLY TUNABLE SEMICONDUCTOR LASER SOURCE FOR OPTICAL FI..(U) CORNELL UNIV ITHACA NY SCHOOL OF ELECTRICAL ENGINEERING C L TANG ET AL. 1/1

UNCLASSIFIED 30 JUL 82 SBI AD-E001 400 N00014-81-C-2050 F/G 20/5 NL

END

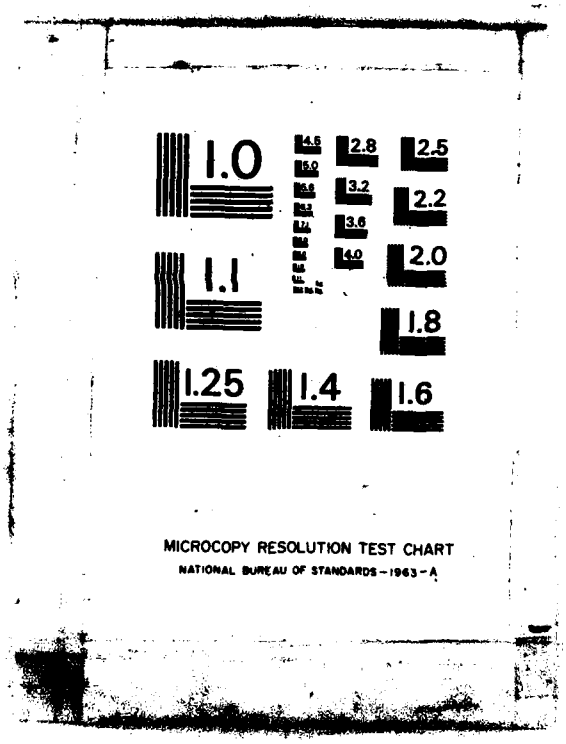
1.0
1.1
1.25
1.4
1.6
2.8
3.2
3.6
4.0
2.5
2.2
2.0
1.8
MICROCOPY RESOLUTION TEST CHART
NATIONAL BUREAU OF STANDARDS - 1963 - A

SCHOOL OF ELECTRICAL ENGINEERING
Cornell University
PHILLIPS HALL
ITHACA, NEW YORK 14853

(2)

July 30, 1982

To: R. Priest, Naval Research Laboratory
From: C. L. Tang
Subject: Final Report on Program on Electrically Tunable Semiconductor Laser Source for Optical Fiber Sensors (Contract N00014-81-C-2050)

STATEMENT OF WORK

The main objective of the program was to develop an electrically tunable semiconductor laser. This laser was to have a smooth tuning curve and is to be electrically tunable over a large spectral range and extremely rapidly tunable. A possible application of such a laser was as the basic tunable laser source of optical fiber sensors.

TASKS COMPLETED

1. An electrically tunable external-cavity semiconductor laser incorporating a Hitachi HLP-1400 laser diode was constructed and delivered to Dr. Ronald Miles of the Naval Research Laboratory on May 7, 1982. With proper alignment, this laser can operate in a single diode mode and can be tuned from single mode to single mode. However, because of the residual reflection at the AR coated intra-cavity surface of the diode, the tuning was not continuous but discrete.

2. A second external-cavity laser with both cleaved facets of the diode AR coated was also constructed (see Fig. 1 for schematic). Continuous electrical tuning was achieved using this laser, but the laser output power was not a smooth function of the wavelength (Fig. 2) due to the residual diode mode structure. Considerable efforts had gone into developing the antireflection coating tech-

nique for semiconductor laser diodes. The final AR coatings on the diode achieved were as nearly perfect as could be achieved with a single quarter-wavelength layer of SiO. The remaining diode mode structure could not, therefore, be eliminated by AR coating the diode facets alone. A different laser structure must be employed. One possible structure is the so-called angle-stripe laser in which the active stripe region is not normal to the cleaved facets of the laser diode.

3. Since angle-striped lasers are not commercially available, a program was established in our laboratory to fabricate such lasers. A liquid-phase-epitaxy system for growing GaAs-$Ga_{1-x}Al_xAs$ double heterostructure lasers was completed. Angle-stripe lasers have been fabricated (see Figs.3 - 6). The threshold of the lasers are at the moment still too high for the applications intended. Work is continuing.

4. In a related project, we have recently also completed a organometallic chemical vapor deposition system for growing semiconductor devices. Excellent GaAs layers have been grown where all the fine structures corresponding to excitons,free and bound to various donors and acceptors, can be clearly resolved. This system will also be available for our semiconductor laser work.

5. Finally, two dynamic interferometric techniques based on electrically tunable lasers were developed and experimentally demonstrated (see Appendix). The first technique allows one to make measurements of small phase modulations in interferometers independent of dc drifts and low frequency noise in the interferometer. The second scheme is a true FM technique suited for continuous noncontact measurements of the optical thickness of transparent materials.

FIGURE CAPTIONS

Figure 1 - Schematic of the external-cavity semiconductor laser with both facets of the laser diode AR coated.

Figure 2 - Solid line: Output power of the laser shown in Fig. 1 vs. wavelength in the scanning mode. Dotted curve: Output power of the laser vs. wavelength when not scanned.

Figure 3 - Light vs. current characteristic of normal-stripe diode laser.

Figure 4 - Light vs. cirrent characteristic of angle-stripe diode laser fabricated from the same wafer as that for the laser shown in Fig. 3.

Figure 5 - Output spectrum of angle-striped laser at low current level.

Figure 6 - Output spectrum of angle-striped laser shown in Fig. 5 at high current level.

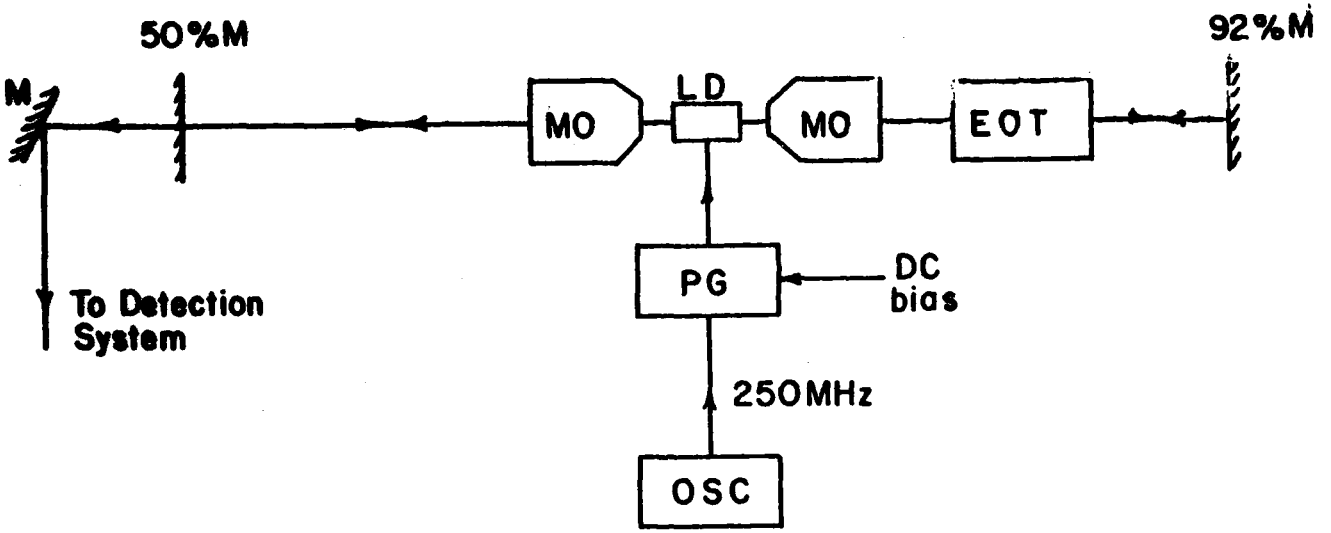
50%M
92%M
M
MO
LD
MO
EOT
To Detection System
PG
DC bias
250MHz
OSC

Figure 1

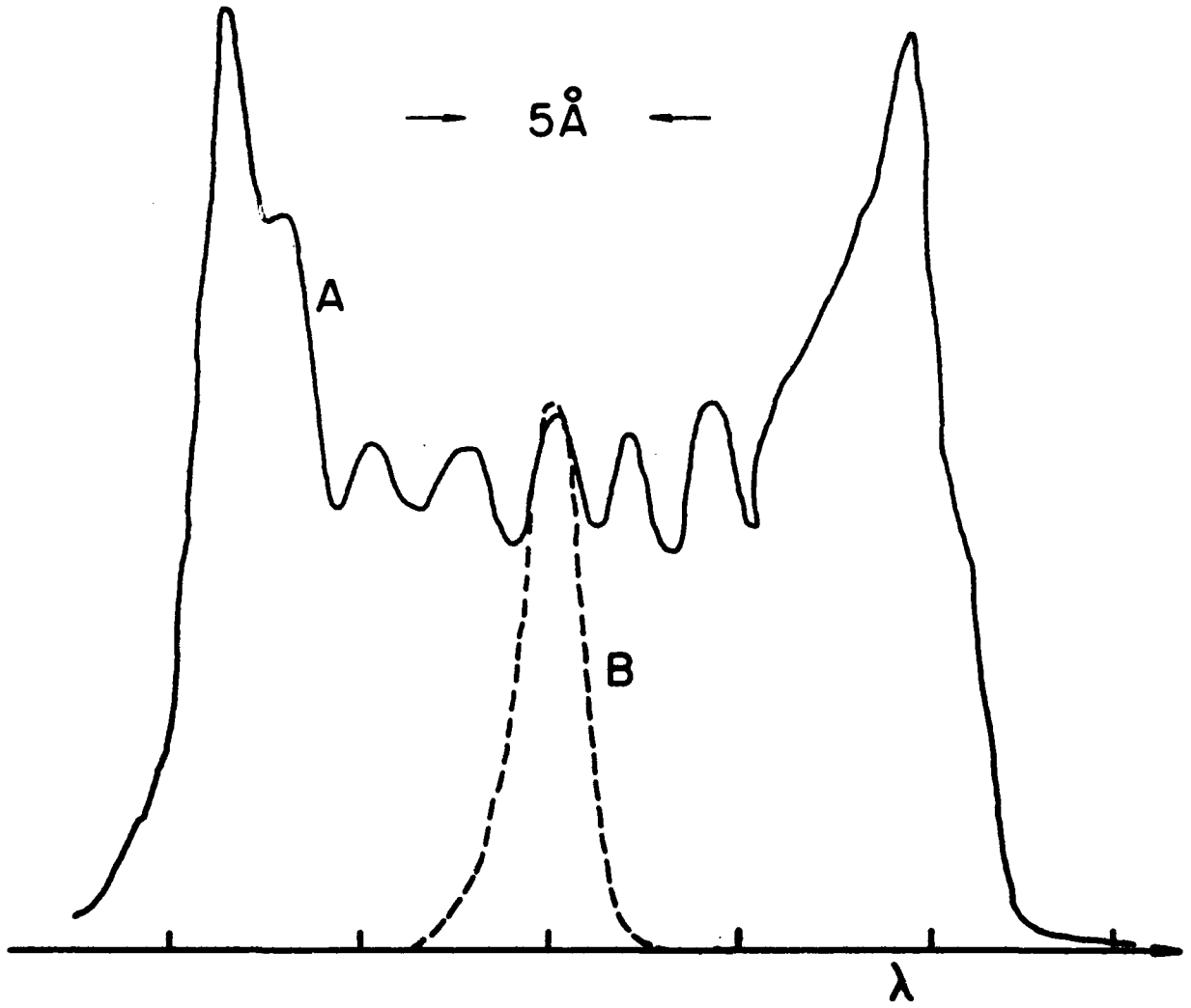

Figure 2

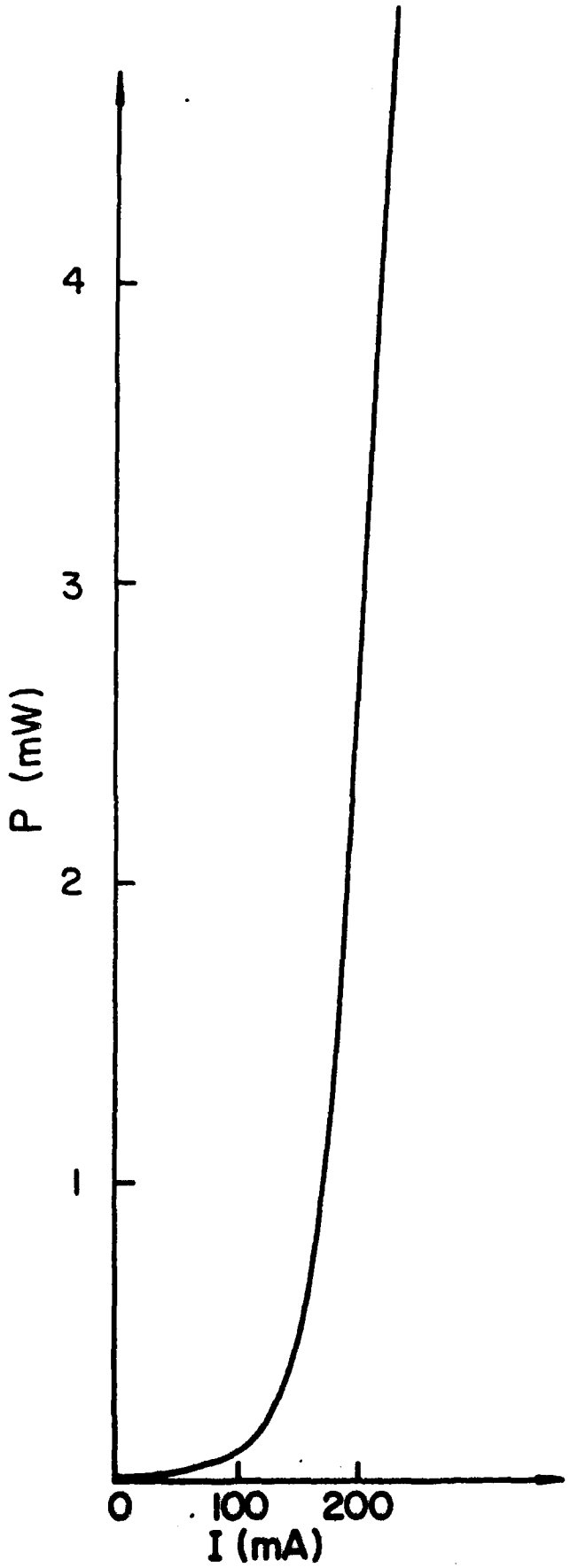

Figure 3

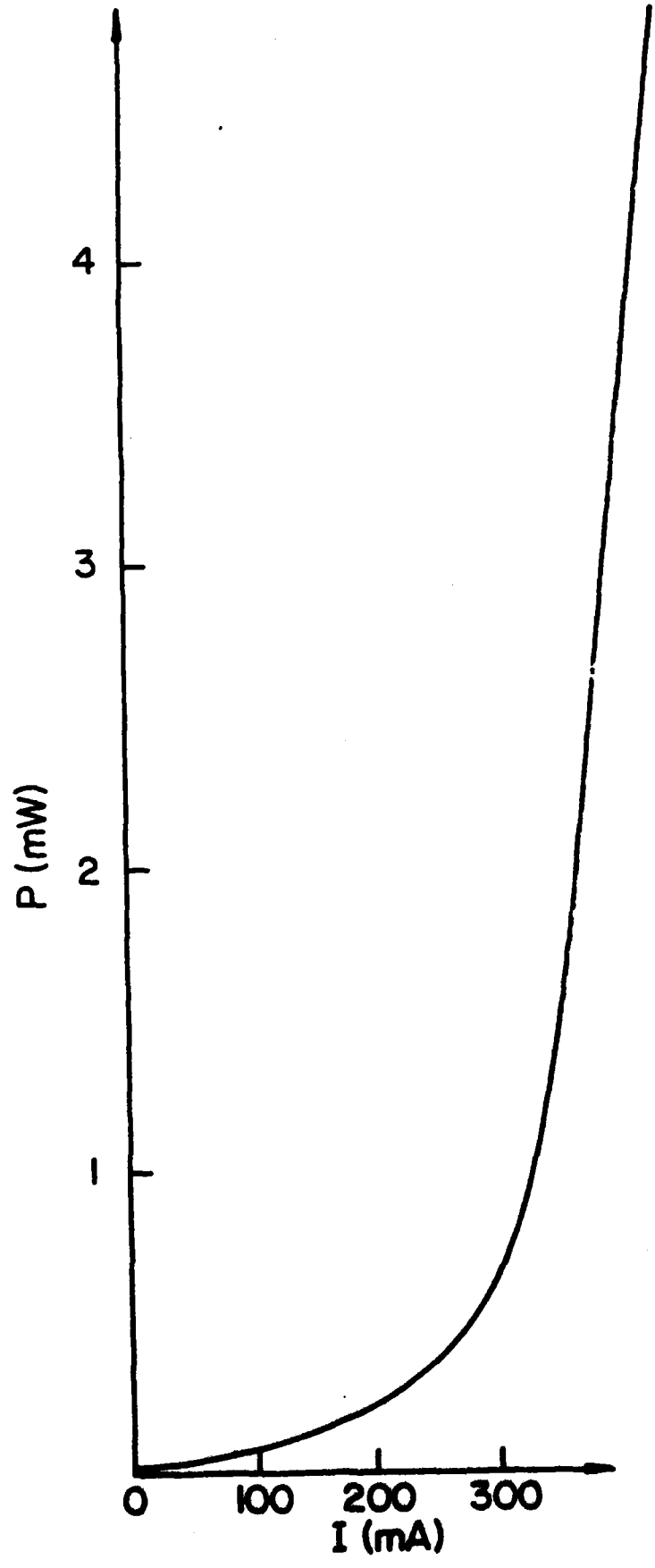
4
3
2
1
P (mW)
0
100
200
300
I (mA)

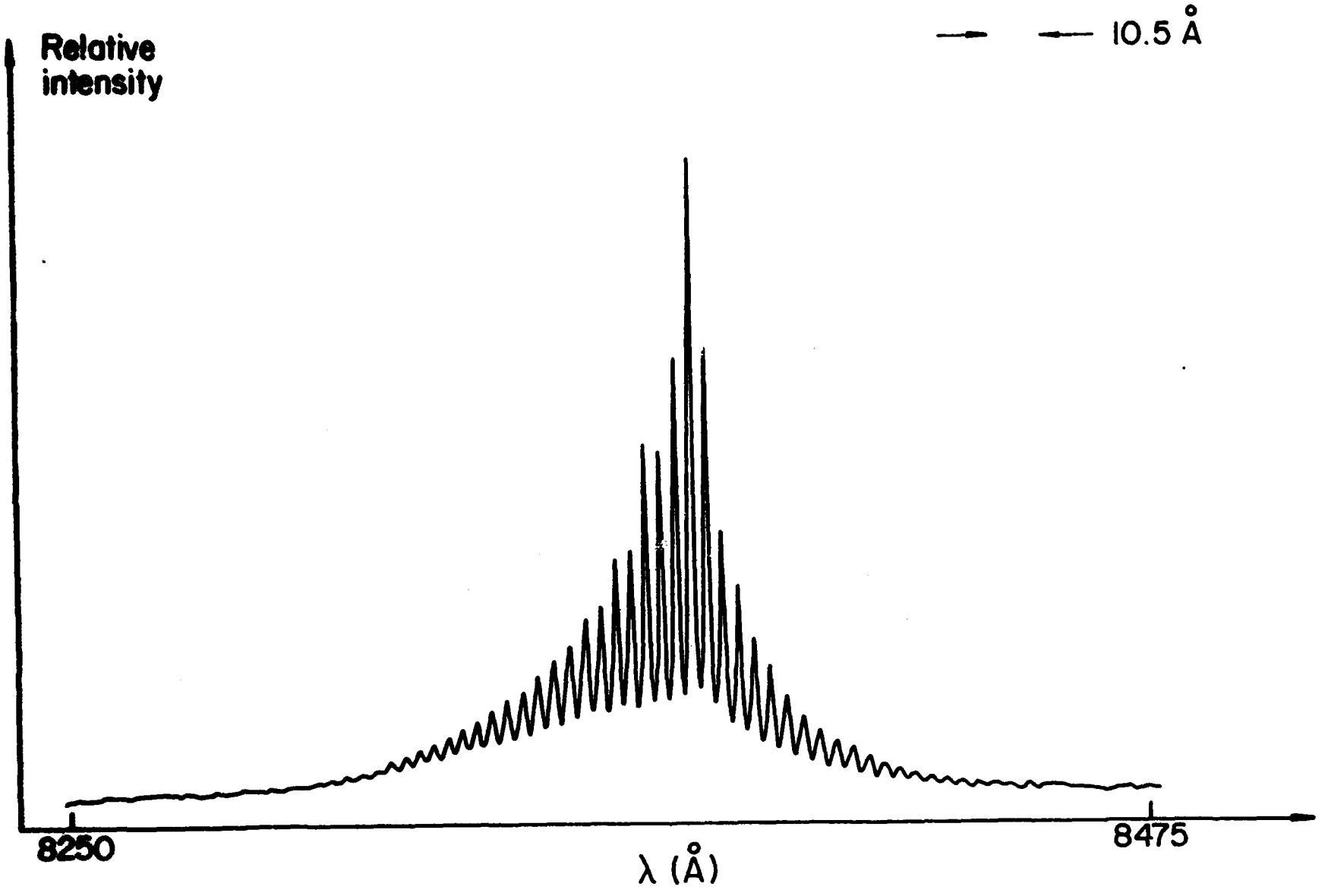

Figure 5

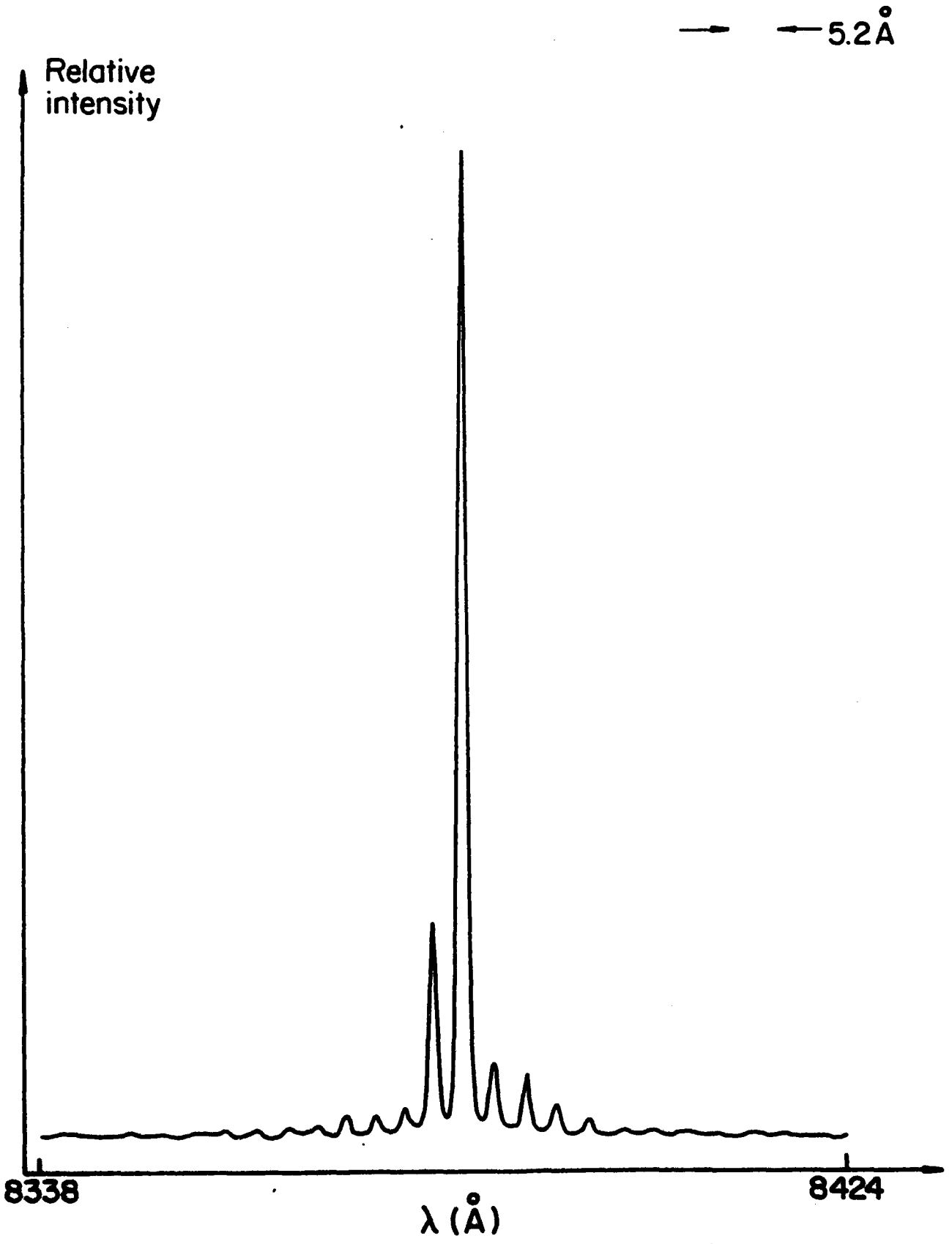

Figure 6

Reprinted from APPLIED OPTICS, Vol. 20, page 3503, October 15, 1981

Dynamic interferometry techniques for optical path length measurements

A. Olsson and C. L. Tang

Two dynamic interferometric techniques based on electrically tunable lasers are described and experimentally demonstrated. The first technique allows for measurements of small phase modulations in interferometers independently of dc drifts and low frequency noise in the interferometer. The second scheme is a true FM technique suited for continuous real-time noncontact measurements of the optical thickness of transparent materials.

I. Introduction

In this paper we describe two dynamic interferometric techniques based on the use of electrically tunable lasers for measuring optical path length and path length changes. In one case it has recently been shown[1] that with the use of a rapidly tunable laser, dc drifts and low frequency phase noise can be eliminated from an interferometer by an active stabilization scheme. Several other authors[2–5] have proposed and demonstrated other feedback schemes to obtain a similar effect. However, in some applications it will not be feasible or even desirable to stabilize the interferometer. For example, if the laser is to drive several independent interferometers, the stabilization scheme of Ref. 1 cannot be used. In the first of the two schemes described in this paper we will show that using a Free Running Interferometric Sensor (FRIS), which incorporates a rapidly tunable laser, it is possible to extract information from the sensor independently of dc drifts and low frequency phase noise. The FRIS system utilizes a passive interferometer, which is desirable in remote sensing applications, and the system also allows for the same laser source to drive several sensors simultaneously.

The second interferometric measurement scheme is a true FM technique, where the information signal is carried in the frequency channel of the detected light signal; it is suited for noncontact real-time measurements of refractive index or length of transparent materials.

The authors are with Cornell University, Ithaca, New York 14853.
Received 9 July 1981.
0003-6935/81/203503-06$00.50/0.

II. Free Running Interferometric Sensor

A. Concept

The basic idea of this scheme is to interrogate an interferometer at two different wavelengths, λ_1 and λ_2, where the difference $\Delta\lambda$ is such that the interferometer outputs at these two wavelengths are in quadrature with respect to each other. With the quadrature component available, a simple vector calculation will give the magnitude of a phase disturbance experienced by the interferometer independently of the absolute phase of the interferometer.

The change ΔS in a signal S derived from the output intensity of a Michelson interferometer due to a small change $\Delta\Phi$ in the phase of the interferometer is given by

$$\Delta S = C \cdot \sin(\Phi)\Delta\Phi, \tag{1}$$

where C is a constant, $\Phi = (2\pi d)/\lambda$ (d being the optical path difference), and λ is the optical wavelength. For two signals, ΔS_1 and ΔS_2, representing the interferometer response at the two wavelengths λ_1 and λ_2 chosen such that $\lambda_1 - \lambda_2 = \lambda^2/(4d)$, Eq. (1) gives

$$\Delta S_1 = C \cdot \sin(\Phi)\Delta\Phi, \tag{2}$$

$$\Delta S_2 = C \cdot \cos(\Phi)\Delta\Phi, \tag{3}$$

$$\Delta\Phi = (1/C)(\Delta S_1^2 + \Delta S_2^2)^{1/2}, \tag{4}$$

where $|\lambda_1 - \lambda_2| \ll \lambda_1 \approx \lambda_2 \equiv \lambda$.

An implementation of the FRIS is shown in Fig. 1. The light source is an electrooptically tuned external cavity GaAlAs semiconductor laser. Several different models of these have been developed in our laboratory and have been described elsewhere.[6,7] By applying a 10-kHz square wave modulation from the pulse generator (PG) onto the intracavity electrooptic tuner (EOT), the laser wavelength is switched between two given

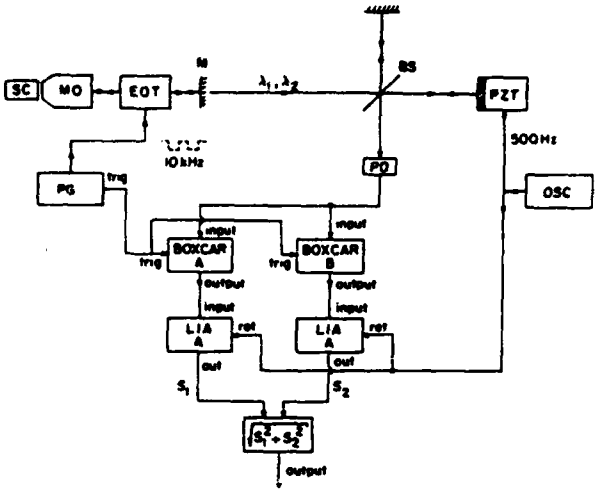

Fig. 1. Schematic of the Free Running Interferometric Sensor: EOT = electrooptic tuner; SC = semiconductor laser diode; MO = microscope objective; M = mirror; BS = beam splitter, PZT = piezoelectric transducer; PG = pulse generator; PD = photodetector, OSC = oscillator; LIA = lock-in amplifier.

wavelengths. The separation between them is typically 3 Å, and the linewidth is ~0.5 Å. The wavelength modulated beam enters a Michelson interferometer in which one mirror is mounted on a piezoelectric transducer (PZT), through which a phase modulation can be introduced in the interferometer. The output from the interferometer is detected with a silicon photodetector/preamp module (PD), and the resulting electrical signal enters two boxcar integrators. The gates of the boxcars are set such that boxcar *A* integrates only when the optical wavelength is λ_1, and boxcar *B* integrates only when the wavelength is λ_2. The length offset between the two arms of the interferometer is initially set such that $2\pi d(\lambda_1 - \lambda_2)/\lambda^2 = \pi/2$, which will ensure that the output signals from the two boxcars are in quadrature. The length adjustment is most easily done by observing the Lissajou pattern between the boxcar outputs when large ($>2\pi$) phase disturbances are introduced into the interferometer. Figure 2(a) shows such a Lissajou figure. The nearly perfect circle shows that the two signals are in quadrature. Figure 2(b) shows the same two signals displayed vs time.

To facilitate measurements of small phase disturbances, two lock-in amplifiers (LIA) were connected to the outputs of the boxcar integrators. The reference signal is derived from the sinusoidal signal applied to the PZT. The analog processor (AP) computes the magnitude of the detected phase modulation in accordance with Eq. (4).

B. Experimental Results

In addition to a small sinusoidal (500-Hz) modulation, a large amplitude triangular signal was applied to the PZT. The triangular signal simulates dc drifts and low frequency noise in the interferometer over several intervals of 2π. The 500-Hz modulation was adjusted to give phase modulations in the 10^{-2}–10^{-4}-rad range.

Figure 3 shows the detected output for phase modulations of (from left) 0, 3.5×10^{-4}, 7.0×10^{-4}, 1.4×10^{-3}, and 2.8×10^{-3} rad (rms). The apparent lack of linearity in Fig. 3 is due solely to poor performance of the AP. The output time constant of the lock-in amplifiers was 10 msec, and the AP had an output time constant of 300 msec. With a 1-sec constant for the AP, the minimum detectable phase modulation at a unity SNR was 7.0×10^{-5} rad (rms). It should be mentioned that no special precautions such as laser amplitude stabilization or mechanical/electrical optimization were taken in obtaining the results presented here. When such steps are taken the minimum detectable phase modulation should be considerably reduced. Sensitivities in the 10^{-6}-rad range should be obtainable as reported by Ref. 8.

Figure 4 shows the Lissajou pattern of the outputs from the lock-in amplifiers for thre different phase modulations: Fig. 4(a) for 2.8×10 ig. 4(b) for 7.0 $\times 10^{-4}$; and Fig. 4(c) for $3.5 \times 10^{-}$ d (rms). Slow

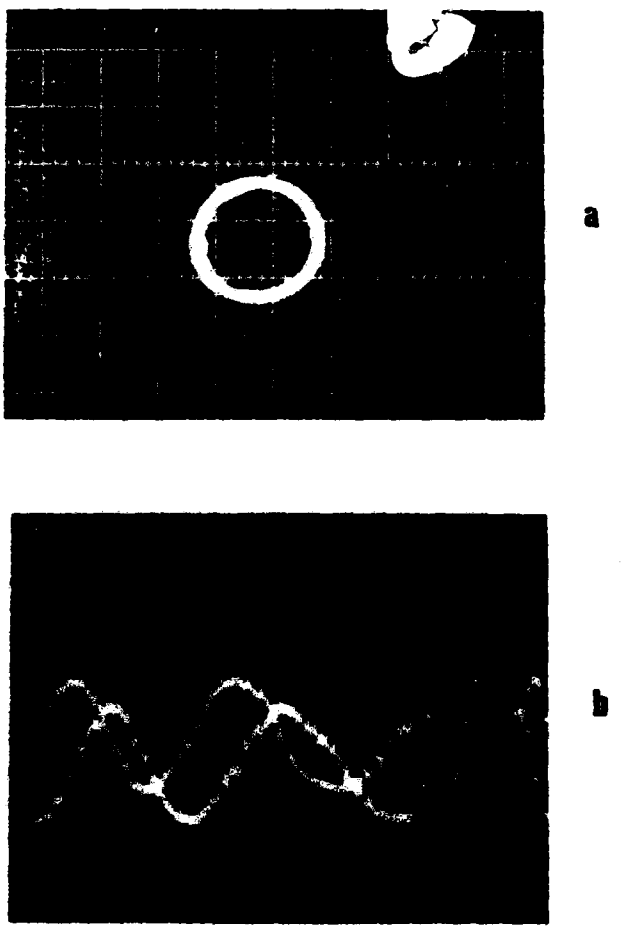

Fig. 2. (a) Lissajou pattern of outputs from the two boxcar integrators when large phase disturbances are present in the interferometer. (b) Same signals as in Fig. 2(a), but displayed vs time. Horizontal scale is 50 msec/div.

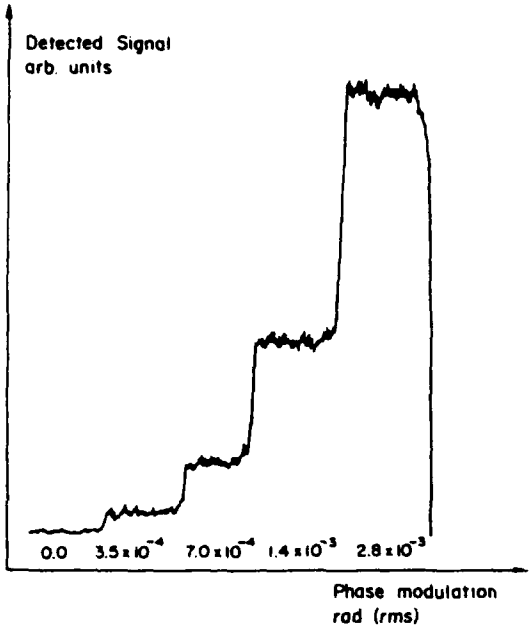

Fig. 3. Detected signal for phase modulations of (from left) 0, 3.5 $\times 10^{-4}$, 7.0 $\times 10^{-4}$, 1.4 $\times 10^{-3}$, and 2.8 $\times 10^{-3}$ rad (rms).

drifts and low frequency phase noise will drive the trajectories in Fig. 4 around the circumference of the circle and hence not degrade the useful signal (radius of the circle). Amplitude noise and phase noise within the signal bandwidth will, however, displace the trajectory radially and will be responsible for the remaining noise in the output signal.

III. Interferometric Optical Thickness Measurement

A. Concept

The second scheme is most suited for continuous measurements of near-static phenomena, where extreme sensitivities are not required. The basic parameter measured is optical thickness, and the method is appropriate to noncontact real-time continuous measurements of length or index of refraction of transparent materials such as glass plates. The basic principle of this scheme is to measure what tuning of the optical wavelength $\Delta\lambda$ is required to change the phase Φ between two interfering beams an integral number N times 2π; these interfering beams, for example, might be the reflected beams from the two surfaces of the glass plate. N, λ, $\Delta\lambda$, and the optical path difference between the two interfering beams d are related by

$$N = \frac{d\Delta\lambda}{\lambda^2}. \tag{5}$$

It should be emphasized that the light intensity, a parameter which is difficult to control and is prone to introduce noise, is not present in Eq. (5). If the laser wavelength is linearly swept with a tuning rate of β Å/sec., Eq. (5) can be replaced by

$$d = \frac{\lambda^2}{T_0\beta}, \tag{6}$$

where T_0 is the time required for cycling the interference phase 2π. Hence, by measuring the period of the intensity variations of the interference of two beams, a measure of the optical path difference is obtained.

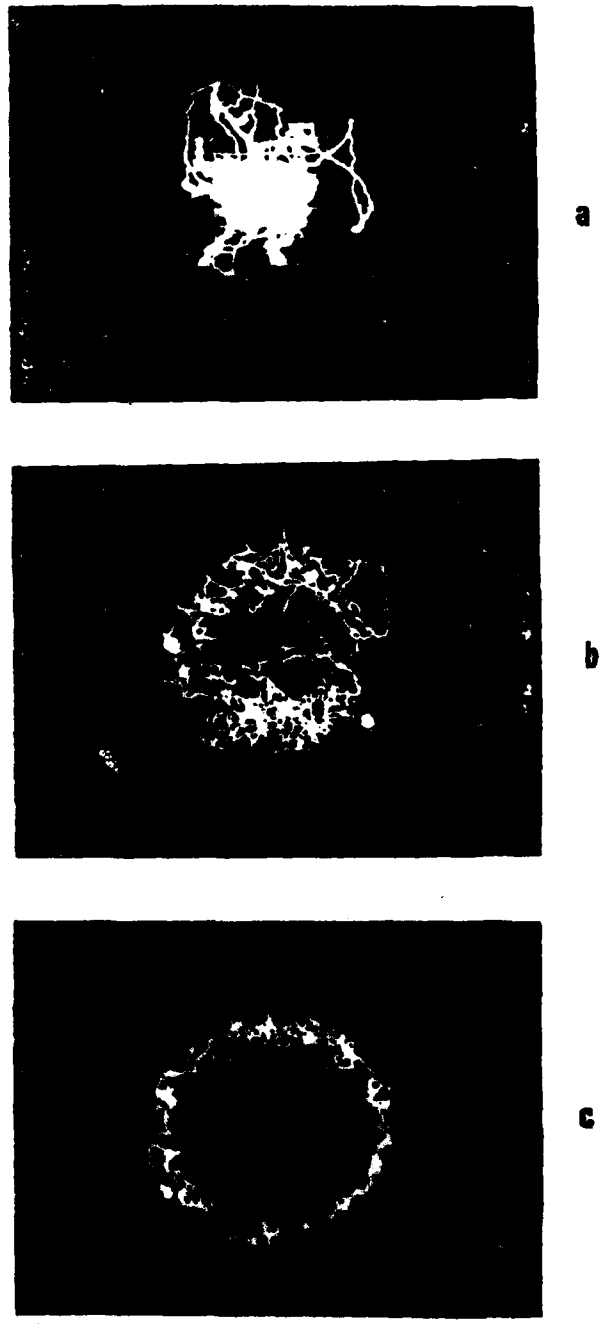

Fig. 4. Lissajou pattern of the outputs from the lock-in amplifiers for phase modulations of (a) 2.8 $\times 10^{-4}$, (b) 7.0 $\times 10^{-4}$, and (c) 3.5 $\times 10^{-3}$ rad (rms). LIA time constant is 10 msec.

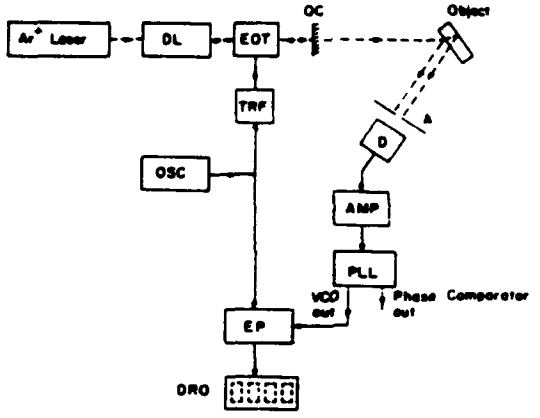

Fig. 5. Schematic of the interferometric thickness monitor: DL = dye laser; EOT = electrooptic tuner; OC = output coupler; TRF = stepup transformer; OSC = oscillator; D = detector; A = aperture; AMP = amplifier; PLL = phase-locked loop circuit; EP = electronic processor; DRO = digital readout.

The experimental setup is shown in Fig. 5. An Ar-ion laser-pumped rhodamine 6G dye laser, which is electronically tuned by the intracavity EOT, was chosen as the light source in this experiment. For experimental convenience the laser wavelength was modulated sinusoidally, and the measurement was made on the linear part of the modulation. The modulation was at 60 Hz and applied to the EOT from an oscillator (OSC) via a stepup transformer (TRF). The peak-to-peak wavelength modulation was ~8 Å. The object whose thickness is to be measured is placed in the beam, and a photodiode samples the interference pattern resulting from the reflections at the front and back surface of the object. A small aperture was inserted in front of the detector to ensure that only a small section of an interference fringe was sampled. After amplification (AMP) the detector signal is processed by a phase-locked loop circuit (PLL). The PLL internal voltage controlled oscillator (VCO) will phase lock to the input frequency. The electronic processor measures the period of the VCO output, and suitable gating derived from the oscillator driving the EOT ensures that the period measurement is done during the linear part of the wavelength modulation. Output is given on a digital display showing the period of the VCO output signal, which is equal to T_0 in Eq. (6). An analog signal proportional to the optical path difference between the two interfering beams can also easily be obtained from the phase comparator output.

B. Experimental Results

To check the performance of this scheme the length offset in a Michelson interferometer was measured. Figure 6 shows the detected waveforms when the length offset is set to (a) 1.3, (b) 2.5, and (c) 5.1 mm. In each figure the top trace is the detector signal, the middle trace is the VCO output, and the lower trace is a pulse burst which lasts for one period of the VCO signal and

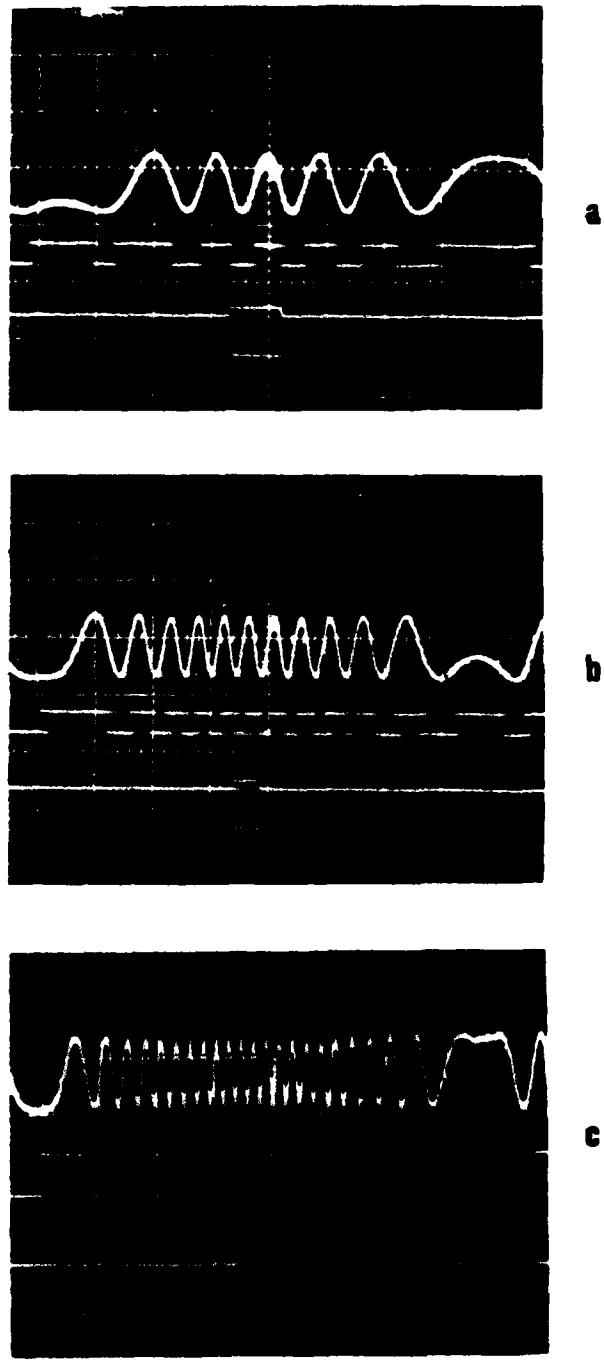

Fig. 6. Detected waveforms for three different optical path length differences: (a) d = 1.3 mm, (b) d = 2.5 mm, and (c) d = 5.1 mm. In each figure the top trace is the detector signal, the middle trace the VCO output from the PLL, and the bottom trace a pulse burst generated in the EP. Width of the pulse burst is proportional to the period of the VCO output signal.

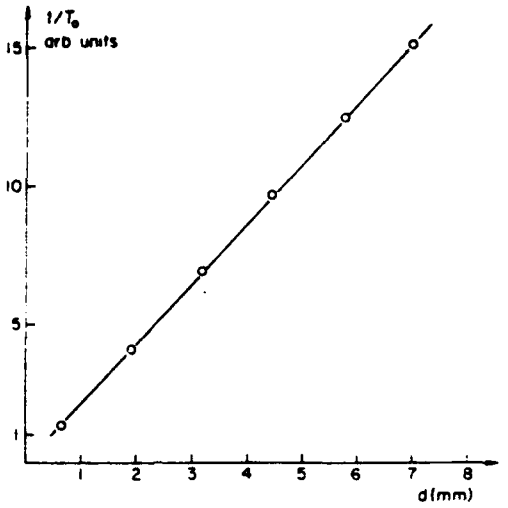

Fig. 7. Measured reciprocal T_0 vs optical path length difference d.

facilitates the period measurement. The individual pulses in the pulse burst are not resolved. Figure 7 shows the measured reciprocal period $1/T_0$ vs length offset in the interferometer. The measurement shows a nonlinearly of <1%. For a given length offset the measured T_0 fluctuates ~0.5%, mainly due to amplitude and frequency instabilities in the oscillator driving the EOT.

The minimum thickness that can be measured with this method is determined by the tuning range of the laser. For a dye laser operating ~6000 Å, with a tuning range of 500 Å, this limit would be of the order of 3 μm. The maximum measurable thickness is limited by the coherence length of the laser. A linewidth of 0.05 Å, which is easily obtainable in dye lasers, would give a maximum measurable thickness of the order of 3 cm. The EOT[9] used in this experiment is ideal for this kind of application, since the linewidth and tuning range can be changed over a wide range by a simple mechanical realignment. The ratio of tuning range to linewidth is approximately 100:1, which gives the same measurement range for a given setting of the tuner.

IV. Conclusions

In this paper we have demonstrated a new type of interferometeric sensor, the Free Running Interferometric Sensor. The key features of this new scheme are:

(1) use of a passive interferometer, an important feature in remote sensing applications;

(2) possibility of driving several sensors in parallel using only one light source;

(3) total immunity to dc drifts and low frequency phase noise in the interferometer; and

(4) use of an electrooptically tuned external cavity semiconductor laser as the light source in this sensor application has shown the importance and versatility of these recently developed lasers.

A second new interferometeric technique for noncontact measurement of optical thickness has also been demonstrated. Using this light intensity independent technique, optical thickness from a few microns to several centimeters can be measured. Continuous quality and production control of optical fibers and glass plates are possible applications.

We thank T. Stockton and A. Ceruzzi of Laser Diode Labs and T. Tsukada of Hitachi for supplying the laser diodes used in this experiment.

This work was supported by the Naval Research Laboratory and the National Science Foundation. Use was also made of the facilities of the Materials Science Center of Cornell University.

References

1. A. Olsson, C. L. Tang, and E. L. Green, Appl. Opt. 19, 1897 (1980).
2. R. F. Cahill and E. Udd, Opt. Lett. 4, 93 (1979).
3. A. D. Fisher and C. Warde, Opt. Lett. 4, 131 (1979).
4. G. C. Bjorklund, K. Jain, and J. D. Hope, Appl. Phys. Lett. 38, 747 (1981).
5. Ira Jeffry Bush, in *Digest of Conference on Lasers and Electrooptics* (Optical Society of America, Washington, D.C., 1981) paper ThE3; D. Jackson, R. Priest, A. Dandridge, and A. Tveten, Appl. Opt. 19, 2926 (1980).
6. C. L. Tang, V. Kreismanis, and J. M. Ballantyne, Appl. Phys. Lett. 30, 113 (1977).
7. A. Olsson and C. L. Tang, IEEE J. Quantum Electron. QE-15, 1085 (1979).
8. D. A. Jackson, A. Dandridge, and S. K. Sheem, Opt. Lett. 5, 139 (1980).
9. Ithaca Research Corp., Electro-Scan tuner.

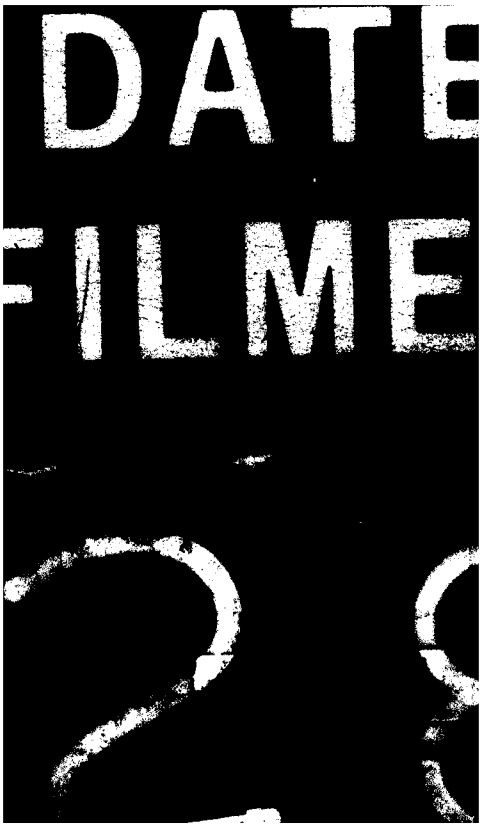
DATE
FILME